

Technical Report: Reactive Planning for Mobile Manipulation Tasks in Unexplored Semantic Environments

Vasileios Vasilopoulos*, Yiannis Kantaros*, George J. Pappas and Daniel E. Koditschek

Abstract—Complex manipulation tasks, such as rearrangement planning of numerous objects, are combinatorially hard problems. Existing algorithms either do not scale well or assume a great deal of prior knowledge about the environment, and few offer any rigorous guarantees. In this paper, we propose a novel hybrid control architecture for achieving such tasks with mobile manipulators. On the discrete side, we enrich a temporal logic specification with mobile manipulation primitives such as moving to a point, and grasping or moving an object. Such specifications are translated to an automaton representation, which orchestrates the physical grounding of the task to mobility or manipulation controllers. The grounding from the discrete to the continuous reactive controller is online and can respond to the discovery of unknown obstacles or decide to push out of the way movable objects that prohibit task accomplishment. Despite the problem complexity, we prove that, under specific conditions, our architecture enjoys provable completeness on the discrete side, provable termination on the continuous side, and avoids all obstacles in the environment. Simulations illustrate the efficiency of our architecture that can handle tasks of increased complexity while also responding to unknown obstacles or unanticipated adverse configurations.

I. INTRODUCTION

Task and motion planning for complex manipulation tasks, such as rearrangement planning of multiple objects, has recently received increasing attention [1]–[3]. However, existing algorithms are typically combinatorially hard and do not scale well, while they also focus mostly on *known* environments [4], [5]. As a result, such methods cannot be applied to scenarios where the environment is initially unknown or needs to be reconfigured to accomplish the assigned mission and, therefore, online replanning may be required, resulting in limited applicability.

Instead, we propose an architecture for addressing complex mobile manipulation task planning problems which can handle unanticipated conditions in unknown environments. Fig. 1 illustrates the problem domain and scope of our algorithm. Fig. 2 illustrates the structure of the architecture and the organization of the paper. Our extensive simulation study suggests that this formal interface between a symbolic logic task planner and a physically grounded dynamical controller - each endowed with their own formal properties - can achieve computationally efficient rearrangement of

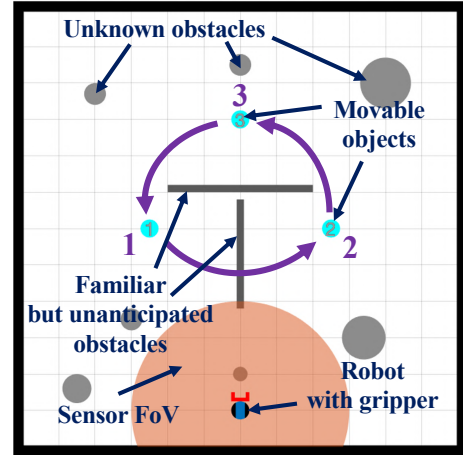


Fig. 1: An example of a task considered in this paper, whose execution is depicted in Fig. 5. A differential drive robot, equipped with a gripper (red) and a limited range onboard sensor for localizing obstacles (orange), needs to accomplish a mobile manipulation task specified by a Linear Temporal Logic (LTL) formula, in a partially known environment (black), cluttered with both unanticipated (dark grey) and completely unknown (light grey) fixed obstacles. Here the task is to rearrange the movable objects counterclockwise, in the presence of the fixed obstacles. Objects’ abstract locations (relative to abstract, named regions of the workspace) are known by the symbolic controller both à-priori and during the entire task sequence. Geometrically complicated obstacles are assumed to be familiar but unanticipated in the sense that neither their number nor placement are known in advance. Completely unknown obstacles are presumed to be convex. All obstacles and disconnected configurations caused by the movable objects are handled by the reactive vector field motion planner (Fig. 2) and never reported to the symbolic controller.

complicated workspaces, motivating work now in progress to give conditions under which their interaction can guarantee success.

A. Mobile Manipulation of Movable Objects

Planning the rearrangement of movable objects has long been known to be algorithmically hard (PSPACE-hardness was established in [7]), and most approaches have focused on simplified instances of the problem. For example, past work on reactive rearrangement using vector field planners such as navigation functions [8] assumes either that each object is actuated [9], [10] or that there are no other obstacles in the environment [11]–[13]. When considering more complicated workspaces, most approaches focus either on sampling-based methods that empirically work well [14], motivated by the typically high dimensional configuration spaces arising from combined task and motion planning [1], [3], or learning a symbolic language on the fly [15]. Such methods can achieve asymptotic optimality [16] by leveraging tools for efficient search on large graphs [17], but come with no guarantee of task completion under partial prior knowledge

* Equal contribution.

The authors are with the GRASP Lab, University of Pennsylvania, Philadelphia, PA 19104. {vvasilo, kantaros, pappasg, kod}@seas.upenn.edu

This work was supported by AFRL grant FA865015D1845 (subcontract 669737-1), AFOSR grant FA9550-19-1-0265 (Assured Autonomy in Contested Environments), and ONR grant #N00014-16-1-2817, a Vannevar Bush Fellowship held by the last author, sponsored by the Basic Research Office of the Assistant Secretary of Defense for Research and Engineering.

recent physical implementations [6], [33] whereby a sensor of range R recognizes and instantaneously localizes any fixed “familiar” or “unfamiliar” obstacles; see also Fig. 1.

The workspace is cluttered by a finite collection of disjoint obstacles of unknown number and placement, denoted by $\tilde{\mathcal{O}}$. This set might also include non-convex “intrusions” of the boundary of the physical workspace \mathcal{W} into the convex hull of the closure of the workspace \mathcal{W} , defined as the *enclosing workspace*. As in [6], [33], [34], we define the *freespace* \mathcal{F} as the set of collision-free placements for the closed ball $\overline{\mathbb{B}(\mathbf{x}, r)}$ centered at \mathbf{x} with radius r , and the *enclosing freespace*, \mathcal{F}_e , as $\mathcal{F}_e := \{\mathbf{x} \in \mathbb{R}^2 \mid \mathbf{x} \in \text{Conv}(\overline{\mathcal{F}})\}$.

Although none of the positions of any obstacles in $\tilde{\mathcal{O}}$ are a-priori known, a subset $\tilde{\mathcal{P}} \subseteq \tilde{\mathcal{O}}$ of these obstacles is assumed to be “familiar” in the sense of having a recognizable polygonal geometry, that the robot can instantly identify and localize (as we have implemented in [6], [33]). The remaining obstacles in $\tilde{\mathcal{C}} := \tilde{\mathcal{O}} \setminus \tilde{\mathcal{P}}$ are assumed to be strongly convex according to [34, Assumption 2] (and implemented in [6], [33]), but are otherwise completely unknown.

To simplify the notation, we dilate each obstacle and movable object by r (or $r + \rho_i$ when the robot carries an object i), and assume that the robot operates in the freespace \mathcal{F} . We denote the set of dilated objects and obstacles derived from $\tilde{\mathcal{M}}, \tilde{\mathcal{O}}, \tilde{\mathcal{P}}$ and $\tilde{\mathcal{C}}$, by $\mathcal{M}, \mathcal{O}, \mathcal{P}$ and \mathcal{C} respectively. For our formal results, we assume that each obstacle in \mathcal{C} is always well-separated from all other obstacles in both \mathcal{C} and \mathcal{P} , as outlined in [6, Assumption 1]; in practice, the surrounding environment often violates our separation assumptions, without precluding successful task completion.

B. Specifying Complex Manipulation Tasks

The robot needs to accomplish a mobile manipulation task, by visiting known regions of interest $\ell_j \subseteq \mathcal{W}$, where $j \in \{1, \dots, L\}$, for some $L > 0$, and applying one of the following three manipulation actions $a_k(M_i, \ell_j) \in \mathcal{A}$, with $M_i \in \mathcal{M}$ referring to a movable object, defined as follows:

- **MOVE**(ℓ_j) instructing the robot to move to region ℓ_j , labeled as $a_1(\emptyset, \ell_j)$, where \emptyset means that this action does not logically entail interaction with any specific movable object¹.
- **GRASPOBJECT**(M_i) instructing the robot to grasp the movable object M_i , labeled as $a_2(M_i, \emptyset)$, with \emptyset denoting that no region is associated with this action.
- **RELEASEOBJECT**(M_i, ℓ_j) instructing the robot to push the (assumed already grasped) object M_i toward its designated goal position, ℓ_j , labeled as $a_3(M_i, \ell_j)$.

For instance, consider a rearrangement planning scenario where the locations of three objects of interest need to be rearranged, as in Fig. 1. We capture such complex manipulation tasks via Linear Temporal Logic (LTL) specifications. Specifically, we use atomic predicates of the form $\pi^{a_k(M_i, \ell_j)}$, which are true when the robot applies the action

$a_k(M_i, \ell_j)$ and false until the robot achieves that action. Note that these atomic predicates allow us to specify temporal logic specifications defined over manipulation primitives and, unlike related works [5], [35], are entirely agnostic to the geometry of the environment. We define LTL formulas by collecting such predicates in a set \mathcal{AP} of atomic propositions. For example, the rearrangement planning scenario with three movable objects initially located in regions ℓ_1, ℓ_2 , and ℓ_3 , as shown in Fig. 1, can be described as a sequencing task [36] by the following LTL formula:

$$\begin{aligned} \phi = & \diamond(\pi^{a_2(M_1, \emptyset)} \wedge \diamond(\pi^{a_3(M_1, \ell_2)} \wedge \\ & \diamond(\pi^{a_2(M_2, \emptyset)} \wedge \diamond(\pi^{a_3(M_2, \ell_3)} \wedge \\ & \diamond(\pi^{a_2(M_3, \emptyset)} \wedge \diamond(\pi^{a_3(M_3, \ell_1)})))))) \end{aligned} \quad (1)$$

where \diamond and \wedge refer to the ‘eventually’ and ‘AND’ operator. In particular, this task requires the robot to perform the following steps in this order (i) grasp object M_1 and release it in location ℓ_2 (first line in (1)); (ii) then grasp object M_2 and release it in location ℓ_3 (second line in (1)); (iii) grasp object M_3 and release it in location ℓ_1 (third line in (1)). LTL formulas are satisfied over an infinite sequence of states [37]. Unlike related works where a state is defined to be the robot position, e.g., [28], here a state is defined by the manipulation action $a_k(M_i, \ell_j)$ that the robot applies. In other words, an LTL formula defined over manipulation-based predicates $\pi^{a_k(M_i, \ell_j)}$ is satisfied by an infinite sequence of actions $p = p_0, p_1, \dots, p_n, \dots$, where $p_n \in \mathcal{A}$, for all $n \geq 0$ [37]. Given a sequence p , the syntax and semantics of LTL can be found in [37]; hereafter, we exclude the ‘next’ operator from the syntax, since it is not meaningful for practical robotics applications [38], as well as the negation operator².

C. Problem Statement

Given a task specification captured by an LTL formula ϕ , our goal is to (i) generate online, as the robot discovers the environment via sensor feedback, appropriate actions using the (discrete) symbolic controller, (ii) translate them to point navigation tasks, (iii) execute these navigation tasks and apply the desired manipulation actions with a (continuous-time) vector field controller, while avoiding unknown and familiar obstacles, (iv) be able to online detect freespace disconnections that prohibit successful action completion, and (v) either locally amend the provided plan by disassembling blocking movable objects, or report failure to the symbolic controller and request an alternative action.

III. SYMBOLIC CONTROLLER

In this Section, we design a discrete controller that generates manipulation commands online in the form of the actions defined in Section II (e.g., ‘release the movable object M_i at a region ℓ_j ’). A summary of the overall architecture is given in Fig. 2, and we now proceed to outline the manner in which

¹Although, as will be detailed in Section V, the hybrid reactive controller may actually need to move objects out of the way, rearranging the topology of the workspace in a manner hidden from the logical task controller.

²Since the negation operator is excluded, safety requirements, such as obstacle avoidance, cannot be captured by the LTL formula; nevertheless, the proposed method can still handle safety constraints by construction of the (continuous-time) reactive, vector field controller in Section V.

the symbolic controller depicted there extends prior work [39] to account for the manipulation-based atomic predicates defined in Section II and adapted to the single-agent setting. The detailed construction can be found in Appendix I.

A. Construction of the Symbolic Controller

First, we translate the specification ϕ , constructed using a set of atomic predicates \mathcal{AP} , into a Non-deterministic Büchi Automaton (NBA) with state-space and transitions among states that can be used to measure how much progress the robot has made in terms of accomplishing the assigned mission; see Appendix I. Particularly, we define a distance metric over this NBA state-space to compute how far the robot is from accomplishing its assigned task, or more formally, from satisfying the accepting condition of the NBA, by following a similar analysis as in [39], [40]. This metric is used to generate manipulation commands online as the robot navigates the unknown environment. Namely, as the robot navigates the workspace, the main idea is that, given its current NBA state, it should reach a next NBA state so that the distance to a state that accomplishes the assigned task decreases over time. Once the target NBA state is selected, a symbolic action is generated in the form of a manipulation action presented in Section II (e.g., ‘release the movable object M_i in region ℓ_j ’) that, once executed, the desired NBA state is reached. This symbolic action acts as an input to the continuous-time controller; see Section V. Observe that the symbolic controller is agnostic to the geometry of the environment; the continuous-time controller is responsible for accomplishing the generated symbolic commands.

When the continuous-time controller accomplishes the assigned sub-task, a new target automaton state is selected and a new manipulation command is generated. In case the continuous-time controller fails to accomplish the assigned sub-task (because e.g., a target region of interest is surrounded by fixed obstacles), the symbolic controller checks if there exists an alternative command that ensures reachability of the target automaton state (e.g., consider a case where a given target NBA state can be reached if the robot goes to either region ℓ_1 or ℓ_2). If there are no alternative commands to reach the desired automaton state, then a new target automaton state is selected that also decreases the distance to satisfying the accepting NBA condition. If there are no other automaton states that can decrease this distance, a message is returned stating that the robot cannot accomplish the assigned mission. A detailed description for the construction of this distance metric is provided in Appendix I.

B. Completeness of the Symbolic Controller

Here, we provide conditions under which the proposed discrete controller is complete. The proof for the following Proposition can be found in Appendix I.

Proposition 1 (Completeness) *Assume that there exists at least one infinite sequence of manipulation actions in the set \mathcal{A} that satisfies ϕ . If the environmental structure and the continuous-time controller always ensure that at least one of the candidate next NBA states can be reached, then*

*the proposed discrete algorithm is complete, i.e., a feasible solution will be found.*³

IV. INTERFACE LAYER BETWEEN THE SYMBOLIC AND THE REACTIVE CONTROLLER

We assume that the robot is nominally in an *LTL mode*, where it executes sequentially the commands provided by the symbolic controller described in Section III. We use an *interface layer* between the symbolic controller and the reactive motion planner, as shown in Fig. 2, to translate each action to an appropriate gripper command ($g = 0$ for MOVE and GRASPOBJECT, and $g = 1$ for RELEASEOBJECT), and a navigation command toward a target \mathbf{x}^* . If the provided action is MOVE(ℓ_j) or RELEASEOBJECT(M_i, ℓ_j), we pick as \mathbf{x}^* the centroid of region ℓ_j . If the action is GRASPOBJECT(M_i), we pick as \mathbf{x}^* a collision-free location on the boundary of object M_i , contained in the freespace \mathcal{F} .

Consider again the example shown in Fig. 1. The first step of the assembly requires the robot to move object M_1 to ℓ_2 which, however, is occupied by the object M_2 . In this case, instead of reporting that the assigned LTL formula cannot be satisfied, we allow the robot to temporarily pause the command execution from the symbolic controller and switch to a *Fix mode* and push object M_2 away from ℓ_1 , before resuming the execution of the action instructed by the symbolic controller. For plan fixing purposes, we introduce a fourth action, DISASSEMBLEOBJECT(M_i, \mathbf{x}^*), invisible to the symbolic controller, instructing the robot to push the object M_i (after it has been grasped using GRASPOBJECT) toward a position \mathbf{x}^* on the boundary of the freespace until specific separation conditions are satisfied. Hence, an additional responsibility of the interface layer (when in *Fix mode*) is to pick the next object to be grasped and disassembled from a stack of blocking movable objects $\mathcal{B}_{\mathcal{M}}$, as well as the target \mathbf{x}^* of each DISASSEMBLEOBJECT action, until the stack $\mathcal{B}_{\mathcal{M}}$ becomes empty⁴; see Section V-B.

Finally, the interface layer (a) requests a new action from the symbolic controller, if the robot successfully converges to \mathbf{x}^* to complete the current action execution, or (b) reports that the currently executed action $a_k(M_i, \ell_j)$ (associated with a movable object M_i and a region of interest ℓ_j) is infeasible and requests an alternative action, if the topology checking module outlined in Section V-A determines that the goal \mathbf{x}^* is surrounded by fixed obstacles.

V. SYMBOLIC ACTION IMPLEMENTATION

In this Section, we describe the online implementation of our symbolic actions, assuming that the robot has already

³Given the current NBA state, denoted by $q_B(t)$, the symbolic controller selects as the next NBA state, a state that is reachable from $q_B(t)$ and closer to the final states as per the proposed distance metric; see also Appendix I. All NBA states that satisfy this condition are called candidate next NBA states. Also, reaching an NBA state means that at least one of the manipulation actions required to enable the transition from $q_B(t)$ to the next NBA state is feasible.

⁴The exclusion of the negation operator from the LTL syntax, as assumed in Section II, guarantees that each DISASSEMBLEOBJECT action will *not* interfere with the satisfaction of the LTL formula ϕ , e.g., the robot will not disassemble an object that should not be grasped or moved.

picked a target \mathbf{x}^* using the interface layer from Section IV. As reported above, in the LTL mode, the robot executes commands from the symbolic controller, using one of the actions MOVE, GRASPOBJECT and RELEASEOBJECT. The robot exits the LTL mode and enters the Fix mode when one or more movable objects block the target destination \mathbf{x}^* ; in this mode, it attempts to rearrange blocking movable objects using a sequence of the actions GRASPOBJECT and DISASSEMBLEOBJECT, before returning to the LTL mode.

The “backbone” of the symbolic action implementation is the reactive, vector field motion planner from prior work [6], allowing either a fully actuated or a differential-drive robot to provably converge to a designated fixed target while avoiding all obstacles in the environment. When the robot is gripping an object i , we use the method from [41] for generating virtual commands for the center $\mathbf{x}_{i,c}$ of the circumscribed disk with radius $(\rho_i + r)$, enclosing the robot and the object. Namely, we assume that the robot-object pair is a fully actuated particle with dynamics $\dot{\mathbf{x}}_{i,c} = \mathbf{u}_{i,c}(\mathbf{x}_{i,c})$, design our control policy $\mathbf{u}_{i,c}$ using the same vector field controller, and translate to commands $\bar{\mathbf{u}} = (v, \omega)$ for our differential drive robot as $\bar{\mathbf{u}} := \mathbf{T}_{i,c}(\psi)^{-1} \mathbf{u}_{i,c}$, with $\mathbf{T}_{i,c}(\psi)$ the Jacobian of the gripping contact, i.e., $\dot{\mathbf{x}}_{i,c} = \mathbf{T}_{i,c}(\psi) \bar{\mathbf{u}}$.

This reactive controller assumes that a path to the goal always exists (i.e., the robot’s freespace is path-connected), and does not consider cases where the target is blocked either by a fixed obstacle or a movable object⁵. Hence, here we extend the algorithm’s capabilities by providing a topology checking algorithm (Section V-A) that detects blocking movable objects or fixed obstacles, as outlined in Fig. 2. Based on these capabilities, Section V-B describes our symbolic action implementations. Appendix II includes a brief overview of the reactive, vector field motion planner, and Appendix III includes an algorithmic outline of our topology checking algorithm.

A. Topology Checking Algorithm

The topology checking algorithm is used to detect freespace disconnections, update the robot’s enclosing freespace \mathcal{F}_e , and modify its action by switching to the Fix mode, if necessary. In summary, the algorithm’s input is the initially assumed polygonal enclosing freespace \mathcal{F}_e for either the robot or the robot-object pair, along with all known dilated movable objects in \mathcal{M} and fixed obstacles in $\mathcal{P}_{\mathcal{I}}$ (corresponding to the index set \mathcal{I} of localized familiar obstacles). The algorithm’s output is the detected enclosing freespace \mathcal{F}_e , used for the diffeomorphism construction in the reactive controller [6], along with a stack of *blocking movable objects* $\mathcal{B}_{\mathcal{M}}$ and a Boolean indication of whether the current symbolic action is feasible. Based on this output, the robot switches to the Fix mode when the stack $\mathcal{B}_{\mathcal{M}}$ becomes non-empty, and resumes execution from the symbolic controller once all movable objects in $\mathcal{B}_{\mathcal{M}}$ are disassembled. A detailed description is given in Appendix III.

⁵The possibility of an entirely unknown blocking convex obstacle is precluded by our separation assumptions in Section II.

B. Action Implementation

We are now ready to describe the used symbolic actions. The symbolic action MOVE(ℓ_j) simply uses the reactive controller to navigate to the selected target \mathbf{x}^* , as described in Appendix II. Similarly, the symbolic action GRASPOBJECT(M_i) uses the reactive controller to navigate to a collision-free location on the boundary of object M_i , and then aligns the robot so that its gripper faces the object, in order to get around Brockett’s condition [42]. RELEASEOBJECT(M_i, ℓ_j) uses the reactive controller to design inputs for the robot-object center $\mathbf{x}_{i,c}$ and translates them to differential drive commands through the center’s Jacobian $\mathbf{T}_{i,c}(\psi)$, in order to converge to the goal \mathbf{x}^* .

Finally, the action DISASSEMBLEOBJECT(M_i, \mathbf{x}^*) is identical to RELEASEOBJECT, with two important differences. First, we heuristically select as target \mathbf{x}^* the middle point of the edge of the polygonal freespace \mathcal{F} that maximizes the distance to all other movable objects (except M_i) and all regions of interest ℓ_j . Second, in order to accelerate performance and shorten the resulting trajectories, we stop the action’s execution if the robot-object pair, centered at $\mathbf{x}_{i,c}$ does not intersect any region of interest and the distance of $\mathbf{x}_{i,c}$ from all other objects in the workspace is at least $2(r + \max_{k \in \mathcal{B}_{\mathcal{M}}} \rho_k)$, as this would imply that dropping the object in its current location would not block a next step of the disassembly process. Even though we do not yet report on formal results pertaining to the task sequence in the Fix mode, the DISASSEMBLEOBJECT action maintains formal results of obstacle avoidance and target convergence to a feasible \mathbf{x}^* , using our reactive, vector field controller.

VI. ILLUSTRATIVE SIMULATIONS

In this Section, we implement simulated examples of different tasks in various environments using our architecture, shown in Fig. 2. All simulations were run in MATLAB using ode45, leveraging and enhancing existing presentation infrastructure⁶. The discrete controller and the interface layer are implemented in MATLAB, whereas the reactive controller is implemented in Python and communicates with MATLAB using the standard MATLAB-Python interface. For our numerical results, we assume perfect robot state estimation and localization of obstacles using the onboard sensor, which can instantly identify and localize either the entirety of familiar obstacles or fragments of unknown obstacles within its range⁷. The reader is referred to the accompanying video submission for visual context and additional simulations.

A. Demonstration of local LTL plan fixing

Fig. 3 includes a demonstration of a simple task, encoded in the LTL formula $\phi = \diamond \pi^{a_1(\emptyset, \ell_1)}$, i.e., eventually execute the action MOVE to navigate to region 1, demonstrating how

⁶See https://github.com/KodlabPenn/semnav_matlab.

⁷The reader is referred to [6], [33] for examples of physical realization of such sensory assumptions, using a combination of an onboard camera for obstacle recognition and pose estimation, and a LIDAR sensor for extracting distance to nearby obstacles.

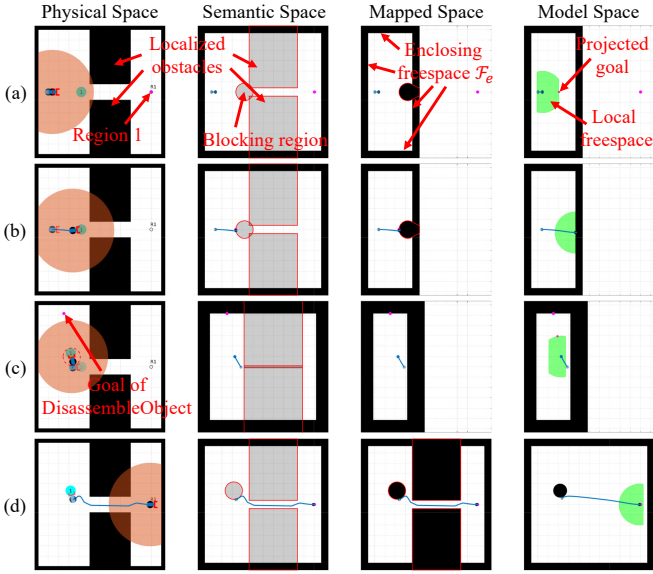


Fig. 3: Demonstration of local LTL plan fixing, where the task is to navigate to region 1, captured by the LTL formula $\phi = \diamond\pi^{a_1(\emptyset, \ell_1)}$ where ℓ_1 refers to region 1 in the figure. (a) The robot starts navigating to its target, until it localizes the two rectangular obstacles and recognizes that the only path to the goal is blocked by a movable object. (b) The robot switches to the Fix mode, grips the object, and (c) moves it away from the blocking region, until the separation assumptions outlined in Section V-B are satisfied. (d) It then proceeds to complete the task.

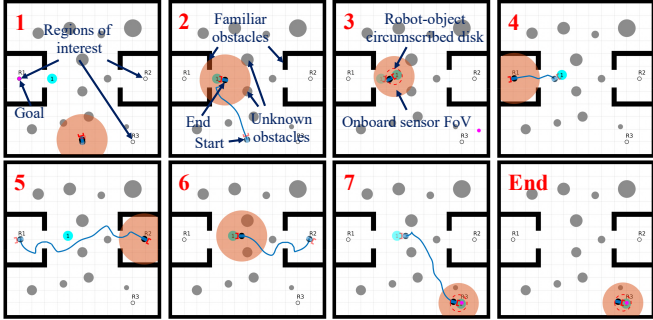


Fig. 4: Executing the LTL formula $\phi = \diamond(\pi^{a_1(\emptyset, \ell_1)} \wedge \diamond(\pi^{a_1(\emptyset, \ell_2)} \wedge \diamond(\pi^{a_2(M_1, \emptyset)} \wedge \diamond\pi^{a_3(M_1, \ell_3)})))$ in an environment cluttered with known walls (black) and unknown convex obstacles (grey).

the Fix mode for local rearrangement of blocking movable objects works.

B. Executing more complex LTL tasks

Fig. 4 includes successive snapshots of a more complicated LTL task, captured by the formula

$$\phi = \diamond(\pi^{a_1(\emptyset, \ell_1)} \wedge \diamond(\pi^{a_1(\emptyset, \ell_2)} \wedge \diamond(\pi^{a_2(M_1, \emptyset)} \wedge \diamond\pi^{a_3(M_1, \ell_3)})))$$

which instructs the robot to first navigate to region 1, then navigate to region 2, and finally grasp object 1 and move it to region 3, in an environment cluttered with both familiar non-convex and completely unknown convex obstacles. Before navigating to region 1, the robot correctly identifies that the movable object disconnects its freespace and proceeds to disassemble it. After visiting region 2, it then revisits the movable object, grasps it and moves it to the designated location to complete the required task. The reader is referred to the video submission for visual context regarding the

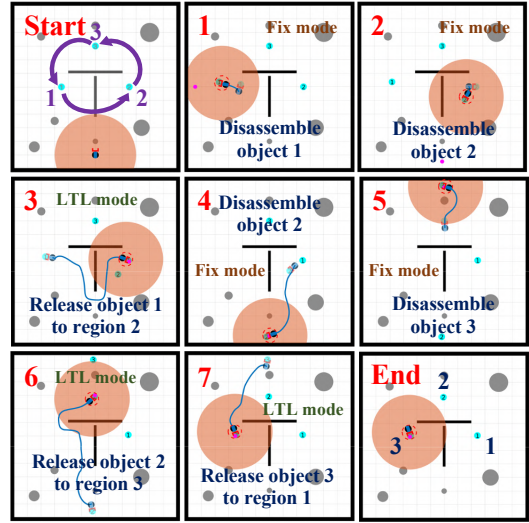


Fig. 5: An illustrative execution of the problem depicted in Fig. 1. The task is specified by the LTL formula (1) requires the counterclockwise rearrangement of 3 objects in an environment cluttered with some unanticipated familiar (initially dark grey and then black upon localization) and some completely unknown (light grey) fixed obstacles.

evolution of all planning spaces [6] (semantic, mapped and model space) during the execution of this task, as well as several other simulations with more movable objects, including (among others) a task where the robot needs to patrol between some predefined regions of interest in an environment cluttered with obstacles by visiting each one of them infinitely often.

C. Execution of rearrangement tasks

Finally, a promising application of our reactive architecture concerns rearrangement planning with multiple movable pieces. Traditionally, such tasks are executed using sampling-based planners, whose offline search times can blow up exponentially with the number of movable pieces in the environment (see, e.g., [18, Table I]). Instead, as shown in Fig. 5, the persistent nature of our reactive architecture succeeds in achieving the given task online in an environment with multiple obstacles, even though our approach might require more steps and longer trajectories in the overall assembly process than other optimal algorithms [16]. Moreover, the LTL formulas for encoding such tasks are quite simple to write (see (1) for the example in Fig. 5), instructing the robot to grasp and release each object in sequence; the reactive controller is capable of handling obstacles and blocking objects during execution time. Our video submission includes a rearrangement example with 4 movable objects, requiring more steps in the assembly process.

VII. CONCLUSION

In this paper, we propose a novel hybrid control architecture for achieving complex tasks with mobile manipulators in the presence of unanticipated obstacles and conditions. Future work will focus on providing end-to-end (instead of component-wise) correctness guarantees, extensions to multiple robots for collaborative manipulation tasks, as well as physical experimental validation.

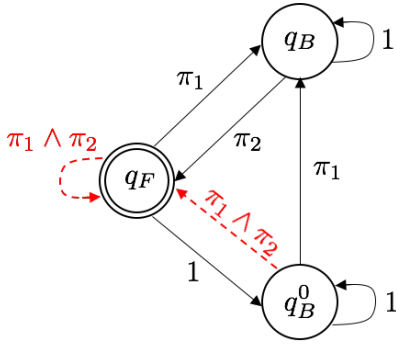


Fig. 6: Graphical illustration of the NBA corresponding to the LTL formula $\phi = \square\Diamond(\pi_1) \wedge \square\Diamond(\pi_2)$ where for simplicity of notation $\pi_1 = \pi^{a_1(\emptyset, \ell_1)}$ and $\pi_2 = \pi^{a_1(\emptyset, \ell_2)}$. The automaton has been generated using the tool in [43]. In words, this LTL formula requires the robot to visit infinitely often and in any order the regions ℓ_1 and ℓ_2 . The initial state of the automaton is denoted by q_B^0 while the final state is denoted by q_F . When the robot is in an NBA state and the Boolean formula associated with an outgoing transition from this NBA state is satisfied, then this transition can be enabled. For instance, when the robot is in the initial state q_B^0 and satisfies the atomic predicate π_1 , the transition from q_B^0 to q_B can be enabled, i.e., $q_B \in \delta_B(q_B^0, \pi_1)$. The LTL formula is satisfied if starting from q_B^0 , the robot generates an infinite sequence of observations (i.e., atomic predicates that become true) that yields an infinite sequence of transitions so that the final state q_F is visited infinitely often. The red dashed lines correspond to infeasible NBA transitions as they are enabled only if the Boolean formula $\pi_1 \wedge \pi_2$ is satisfied, i.e., only if the robot is in more than one region simultaneously; such edges are removed yielding the pruned NBA.

APPENDIX I DETAILED DESCRIPTION OF THE SYMBOLIC CONTROLLER

This Appendix provides a detailed description of the distance metric used in Section III upon which a discrete controller is designed that generates manipulation commands online. To accomplish this, first in Appendix I-A we translate the LTL formula into a Non-deterministic Büchi Automaton (NBA) and we provide a formal definition of its accepting condition. Then, in Appendix I-B, we provide a detailed description for the construction of the distance metric over this automaton state space. Appendix I-C describes our method for generating symbolic actions online, and Appendix I-D includes the proof of our completeness result. The proposed method is also illustrated in Figs. 6-7.

A. From LTL formulas to Automata

As reported in Section III, we first translate the specification ϕ , constructed using a set of atomic predicates \mathcal{AP} , into a Non-deterministic Büchi Automaton (NBA) defined as follows; see also Fig. 6.

Definition 1 (NBA) A Non-deterministic Büchi Automaton (NBA) B over $\Sigma = 2^{\mathcal{AP}}$ is defined as a tuple $B = (\mathcal{Q}_B, \mathcal{Q}_B^0, \delta_B, \mathcal{Q}_F)$, where (i) \mathcal{Q}_B is the set of states; (ii) $\mathcal{Q}_B^0 \subseteq \mathcal{Q}_B$ is a set of initial states; (iii) $\delta_B : \mathcal{Q}_B \times \Sigma \rightarrow 2^{\mathcal{Q}_B}$ is a non-deterministic transition relation, and $\mathcal{Q}_F \subseteq \mathcal{Q}_B$ is a set of accepting/final states.

To interpret a temporal logic formula over the trajectories of the robot system, we use a labeling function $L : \mathcal{A} \rightarrow 2^{\mathcal{AP}}$ that determines which atomic propositions are true

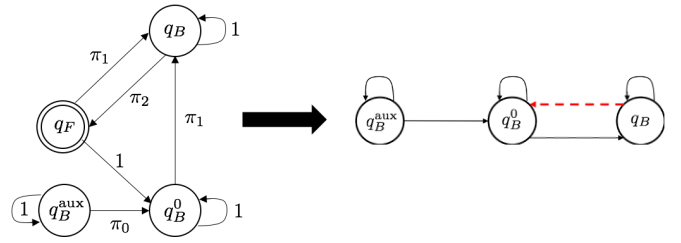


Fig. 7: Graphical illustration of the graph \mathcal{G} construction for the NBA shown in Fig. 6. The left figure corresponds to the pruned automaton after augmenting its state space with the state q_B^{aux} , where π_0 corresponds to the atomic predicate that the robot satisfies initially at $t = 0$. If no atomic predicates are satisfied initially, then π_0 corresponds to the empty symbol [37]. Observe in the left figure that $\mathcal{D}_{q_B^{\text{aux}}} = \{q_B^{\text{aux}}, q_B^0, q_B\}$. The right figure illustrates the graph \mathcal{G} corresponding to this automaton. The red dashed line corresponds to an accepting edge. Also, we have that $\mathcal{V}_F = \{q_B\}$, $d_F(q_B^{\text{aux}}, \mathcal{V}_F) = 2$, $d_F(q_B^0, \mathcal{V}_F) = 1$, and $d_F(q_B, \mathcal{V}_F) = 0$. For instance, every time the robot reaches the state q_B^0 with $d_F(q_B^0, \mathcal{V}_F) = 1$, it generates a symbol to reach the state q_B since reaching this state decreases the distance to the set of accepting edges (since $d_F(q_B, \mathcal{V}_F) = 0$). The symbol that can enable this transition is the symbol that satisfies the Boolean formula $b^{q_B^0, q_B} = \pi_1$; this formula is trivially satisfied by the symbol $\pi_1 = \pi^{a_1(\emptyset, \ell_1)}$. As a result the command sent to the continuous time controller is ‘Move to Region ℓ_1 ’.

given the current robot action $a_k(M_i, \ell_j)$; note that, by definition, these actions also encapsulate the position of the robot in the environment. An infinite sequence $p = p(0)p(1) \dots p(k) \dots$ of actions $p(k) \in \mathcal{A}$, satisfies ϕ if the word $\sigma = L(p(0))L(p(1)) \dots$ yields an accepting NBA run defined as follows [37]. First, a run ρ_B of B over an infinite word $\sigma = \sigma(1)\sigma(2) \dots \sigma(k) \dots \in (2^{\mathcal{AP}})^\omega$, is a sequence $\rho_B = q_B^0 q_B^1 q_B^2 \dots, q_B^k, \dots$, where $q_B^0 \in \mathcal{Q}_B^0$ and $q_B^{k+1} \in \delta_B(q_B^k, \sigma(k))$, $\forall k \in \mathbb{N}$. A run ρ_B is called *accepting* if at least one final state appears infinitely often in it. In words, an infinite-length discrete plan τ satisfies an LTL formula ϕ if it can generate at least one accepting NBA run.

B. Distance Metric Over the NBA

In this Section, given a graph constructed using the NBA, we define a function to compute how far an NBA state is from the set of final states. Following a similar analysis as in [39], [40], we first prune the NBA by removing infeasible transitions that can never be enabled as they require the robot to be in more than one region and/or take more than one action simultaneously. Specifically, a symbol $\sigma \in \Sigma := 2^{\mathcal{AP}}$ is *feasible* if and only if $\sigma \not\models b^{\text{inf}}$, where b^{inf} is a Boolean formula defined as

$$b^{\text{inf}} = [(\bigvee_{k,r,j,e \neq j} (\pi^{a_k(\cdot, \ell_e)} \wedge \pi^{a_r(\cdot, \ell_j)}))] \vee [(\bigvee_{j,k,r \neq k} (\pi^{a_k(\cdot, \ell_j)} \wedge \pi^{a_r(\cdot, \ell_j)}))]. \quad (2)$$

In words, b^{inf} requires the robot to be either present simultaneously in more than one region *or* take more than one action in a given region at the same time. Specifically, the first line requires the robot to be present in locations ℓ_j and ℓ_e , $e \neq j$ and apply the actions $a_k, a_r \in \mathcal{A}$ while the second line requires the robot to take two distinct actions $a_k(\cdot, \ell_j)$ and $a_r(\cdot, \ell_j)$ at the same region ℓ_j , simultaneously.

Next, we define the sets that collect all feasible symbols that enable a transition from an NBA state q_B to another,

not necessarily different, NBA state q'_B . This definition relies on the fact that transition from a state q_B to a state q'_B is enabled if a Boolean formula, denoted by b^{q_B, q'_B} and defined over the set of atomic predicates \mathcal{AP} , is satisfied. In other words, $q'_B \in \delta_B(q_B, \sigma)$, i.e., q'_B can be reached from the NBA state q_B under the symbol σ , if σ satisfies b^{q_B, q'_B} . An NBA transition from q_B to q'_B is infeasible if there are no feasible symbols that satisfy b^{q_B, q'_B} . All infeasible NBA transitions are removed yielding a pruned NBA automaton. All feasible symbols that satisfy b^{q_B, q'_B} are collected in the set Σ^{q_B, q'_B} .

To take into account the initial robot state in the construction of the distance metric, in the pruned automaton we introduce an auxiliary state q_B^{aux} and transitions from q_B^{aux} to all initial states $q_B^0 \in \mathcal{Q}_B^0$ so that $b^{q_B^{\text{aux}}, q_B^0} = 1$ and $b^{q_B^{\text{aux}}, q_B^0} = \pi_0$, i.e., transition from q_B^{aux} to q_B^0 can always be enabled based on the atomic predicate that is initially satisfied denoted by π_0 ; note that if no predicates are satisfied initially, then π_0 corresponds to the empty symbol [37]. Hereafter, the auxiliary state q_B^{aux} is considered to be the initial state of the resulting NBA; see also Fig. 7.

Next, we collect all NBA states that can be reached from q_B^{aux} in a possibly multi-hop fashion, using a finite sequence of feasible symbols, so that once these states are reached, the robot can always remain in them as long as needed using the same symbol that allowed it to reach this state. Formally, let $\mathcal{D}_{q_B^{\text{aux}}}$ be a set that collects all NBA states q_B (i) that have a feasible self-loop, i.e., $\Sigma^{q_B, q_B} \neq \emptyset$ and (ii) for which there exists a finite and feasible word w , i.e., a finite sequence of feasible symbols, so that starting from q_B^{aux} a finite NBA run ρ_w (i.e., a finite sequence of NBA states) is incurred that ends in q_B and activates the self-loop of q_B . In math, $\mathcal{D}_{q_B^{\text{aux}}}$ is defined as:

$$\mathcal{D}_{q_B^{\text{aux}}} = \{q_B \in \mathcal{Q}_B \mid (\Sigma^{q_B, q_B} \neq \emptyset) \wedge (\exists w \text{ s.t. } \rho_w = q_B^{\text{aux}} \dots \bar{q}_B q_B q_B)\}. \quad (3)$$

By definition of q_B^{aux} , we have that $q_B^{\text{aux}} \in \mathcal{D}_{q_B^{\text{aux}}}$.

Among all possible pairs of states in $\mathcal{D}_{q_B^{\text{aux}}}$, we examine which transitions, possibly multi-hop, can be enabled using feasible symbols, so that, once these states are reached, the robot can always remain in them forever using the same symbol that allowed it to reach this state. Formally, consider any two states $q_B, q'_B \in \mathcal{D}_{q_B^{\text{aux}}}$ (i) that are connected through a - possibly multi-hop - path in the NBA, and (ii) for which there exists a symbol, denoted by σ^{q_B, q'_B} , so that if it is repeated a finite number of times starting from q_B , the following finite run can be generated:

$$\rho = q_B q_B^1 \dots q_B^{K-1} q_B^K q_B^K, \quad (4)$$

where $q_B^k = q_B^K$, for some finite $K > 0$. In (4), the run is defined so that (i) $q_B^k \neq q_B^{k+1}$, for all $k \in \{1, K-1\}$; (ii) $q_B^k \in \delta_B(q_B^k, \sigma^{q_B, q'_B})$ is not valid for all $\forall k \in \{1, \dots, K-1\}$, i.e., the robot cannot remain in any of the intermediate states (if any) that connect q_B to q'_B either because a feasible self-loop does not exist or because σ^{q_B, q'_B} cannot activate this self-loop; and (iii) $q'_B \in \delta_B(q'_B, \sigma^{q_B, q'_B})$ i.e., there is a

feasible loop associated with q'_B that is activated by σ^{q_B, q'_B} . Due to (iii), the robot can remain in q'_B as long as σ^{q_B, q'_B} is generated. The fact that the finite repetition of a *single* symbol needs to generate the run (4) precludes multi-hop transitions from q_B to q'_B that require the robot to jump from one region of interest to another one instantaneously as such transitions are not meaningful as discussed in Section II; see also Fig. 7. Hereafter, we denote the - potentially multi-hop - transition incurred due to the run (4) by $q'_B \in \delta_B^m(q_B, \cdot)$.

Then, we construct the directed graph $\mathcal{G} = \{\mathcal{V}, \mathcal{E}\}$ where $\mathcal{V} \subseteq \mathcal{Q}_B$ is the set of nodes and $\mathcal{E} \subseteq \mathcal{V} \times \mathcal{V}$ is the set of edges. The set of nodes is defined so that $\mathcal{V} = \mathcal{D}_{q_B^{\text{aux}}}$ and the set of edges is defined so that $(q_B, q'_B) \in \mathcal{E}$ if there exists a feasible symbol that incurs the run ρ_w defined in (4); see also Fig. 7.

Given the graph \mathcal{G} , we define the following distance metric.

Definition 2 (Distance Metric) Let $\mathcal{G} = \{\mathcal{V}, \mathcal{E}\}$ be the directed graph that corresponds to NBA B . Then, we define the distance function $d: \mathcal{V} \times \mathcal{V} \rightarrow \mathbb{N}$ as follows

$$d(q_B, q'_B) = \begin{cases} |SP_{q_B, q'_B}|, & \text{if } SP_{q_B, q'_B} \text{ exists,} \\ \infty, & \text{otherwise,} \end{cases} \quad (5)$$

where SP_{q_B, q'_B} denotes the shortest path (in terms of hops) in \mathcal{G} from q_B to q'_B and $|SP_{q_B, q'_B}|$ stands for its cost (number of hops).

In words, $d: \mathcal{V} \times \mathcal{V} \rightarrow \mathbb{N}$ returns the minimum number of edges in the graph \mathcal{G} that are required to reach a state $q'_B \in \mathcal{V}$ starting from a state $q_B \in \mathcal{V}$. This metric can be computed using available shortest path algorithms, such the Dijkstra method with worst-case complexity $O(|\mathcal{E}| + |\mathcal{V}| \log |\mathcal{V}|)$.

Next, we define the final/accepting edges in \mathcal{G} as follows.

Definition 3 (Final/Accepting Edges) An edge $(q_B, q'_B) \in \mathcal{E}$ is called final or accepting if the corresponding multi-hop NBA transition $q'_B \in \delta_B^m(q_B, \cdot)$ includes at least one final state $q_F \in \mathcal{Q}_F$.

Based on the definition of accepting edges, we define the set $\mathcal{V}_F \subseteq \mathcal{V}$ that collects all states $q_B \in \mathcal{V}$ from which an accepting edge originates, i.e.,

$$\mathcal{V}_F = \{q_B \in \mathcal{V} \mid \exists \text{ accepting edge } (q_B, q'_B) \in \mathcal{E}\}. \quad (6)$$

By definition of the accepting condition of the NBA, we have that if at least one of the accepting edges is traversed infinitely often, then the corresponding LTL formula is satisfied.

Similar to [44], we define the distance of any state $q_B \in \mathcal{V}$ to the set $\mathcal{V}_F \subseteq \mathcal{V}$ as

$$d_F(q_B, \mathcal{V}_F) = \min_{q'_B \in \mathcal{V}_F} d(q_B, q'_B), \quad (7)$$

where $d(q_B, q'_B)$ is defined in (5) and \mathcal{V}_F is defined in (6); see also Fig. 7.

C. Online symbolic controller

In this Section, we present how manipulation commands are generated online. The proposed controller requires as an input the graph \mathcal{G} defined in Appendix I-B. The main idea is that as the robot navigates the unknown environment, it selects NBA states that it should visit next so that the distance to the final states, as per (7), decreases over time.

Let $q_B(t) \in \mathcal{V}$ be the NBA state that the robot has reached after navigating the unknown environment for t time units. At time $t = 0$, $q_B(t)$ is selected to be the initial NBA state. Given the current NBA state $q_B(t)$, the robot selects a new NBA state, denoted by $q_B^{\text{next}} \in \mathcal{V}$ that it should reach next to make progress towards accomplishing their task. This state is selected among the neighbors of $q_B(t)$ in the graph \mathcal{G} based on the following two cases. If $q_B(t) \notin \mathcal{V}_F$, where \mathcal{V}_F is defined in (6), then among all neighboring nodes, we select one that satisfies

$$d_F(q_B^{\text{next}}, \mathcal{V}_F) = d_F(q_B(t), \mathcal{V}_F) - 1, \quad (8)$$

i.e., a state that is one hop closer to the set \mathcal{V}_F than $q_B(t)$ is where d_F is defined in (7). Under this policy of selecting q_B^{next} , we have that eventually $q_B(t) \in \mathcal{V}_F$; controlling the robot to ensure this property is discussed in Section V. If $q_B(t) \in \mathcal{V}_F$, then the state q_B^{next} is selected so that $(q_B(t), q_B^{\text{next}})$ is an accepting edge as per Definition 3. This way we ensure that accepting edges are traversed infinitely often and, therefore, the assigned LTL task is satisfied.

Given the selected state q_B^{next} , a feasible symbol is selected that can enable the transition from $q_B(t)$ to q_B^{next} , i.e., can incur the run (4). By definition of the run in (4), it suffices to select a symbol that satisfies the following Boolean formula:

$$b^{q_B, q'_B} = b^{q_B, q_B^1} \wedge b^{q_B^2, q_B^3} \wedge \dots \wedge b^{q_B^{K-1}, q_B^K} \wedge b^{q_B^K, q_B^K}, \quad (9)$$

where $q_B^K = q_B^{\text{next}}$. In words, the Boolean formula in (9) is the conjunction of all Boolean formulas $b^{q_B^{k-1}, q_B^k}$ that need to be satisfied simultaneously to reach $q_B^{\text{next}} = q_B^K$ through a multi-hop path. Once such a symbol is generated, a point-to-point navigation and manipulation command is accordingly generated. For instance, if this symbol is $\pi^{a_k(M_i, \ell_j)}$ then the robot has to apply the action $a_k(M_i, \ell_j)$, i.e., go to a known region of interest ℓ_j and apply action a_k to the movable object M_i . The online implementation of such action is discussed in Section V.

D. Completeness of the symbolic controller

In what follows, we provide the proof of Proposition 1.

Proof of Proposition 1. To show this result it suffices to show that eventually the accepting condition of the NBA is satisfied, i.e., the robot will visit at least one of the final NBA states q_F infinitely often. Equivalently, as discussed in Appendix I-B, it suffices to show that accepting edges $(q_B, q'_B) \in \mathcal{E}$, where $q_B, q'_B \in \mathcal{V}$ are traversed infinitely often.

First, consider an infinite sequence of time instants $\mathbf{t} = t_0, t_1, \dots, t_k, \dots$ where $t_{k+1} \geq t_k$, so that an edge in \mathcal{G} , defined in Appendix I-B, is traversed at every time

instant t_k . Let $e(t_k) \in \mathcal{E}$ denote the edge that is traversed at time t_k . Thus, \mathbf{t} yields the following sequence of edges $\mathbf{e} = e(t_0), e(t_1), \dots, e(t_k) \dots$ where $e(t_k) = (q_B(t_k), q_B(t_{k+1}))$, $q_B(t_0) = q_B^{\text{aux}}$, $q_B(t_k) \in \mathcal{V}$, and the state q_B^{k+1} is defined based on the following two cases. If $q_B(t_k) \notin \mathcal{V}_F$, then the state $q_B(t_{k+1})$ is closer to \mathcal{V}_F than $q_B(t_k)$ is, i.e., $d_F(q_B(t_{k+1}), \mathcal{V}_F) = d_F(q_B(t_k), \mathcal{V}_F) - 1$, where d_F is defined in (7). If $q_B(t_k) \in \mathcal{V}_F$, then $q_B(t_{k+1})$ is selected so that an accepting edge originating from $q_B(t_k)$ is traversed. By definition of $q_B(t_k)$, the ‘distance’ to \mathcal{V}_F decreases as t_k increases, i.e., given any time instant t_k , there exists a time instant $t'_k \geq t_k$ so that $q_B(t'_k) \in \mathcal{V}_F$ and then at the next time instant an accepting edge is traversed. This means that \mathbf{e} includes an infinite number of accepting edges. This sequence \mathbf{e} exists since, by assumption, there exists an infinite sequence of manipulation actions that satisfies ϕ . Particularly, recall that by construction of the graph \mathcal{G} , the set of edges in this graph captures all NBA transitions besides those that (i) require the robot to be in more than one region simultaneously or (ii) multi-hop NBA transitions that require the robot to jump instantaneously from one region of interest which are not meaningful in practice. As a result, if there does not exist at least one sequence \mathbf{e} , i.e., at least one infinite path in \mathcal{G} that starts from the initial state and traverses at least one accepting edge infinitely often, then this means that there is no path that satisfies ϕ (unless conditions (i)-(ii) mentioned before are violated).

Assume that the discrete controller selects NBA states as discussed in Appendix I-C. To show that the discrete controller is complete, it suffices to show that it can generate a infinite sequence of edges \mathbf{e} as defined before. Note that the discrete controller selects next NBA states that the robot should reach in the same way as discussed before. Also, by assumption, the environmental structure and the continuous-time controller ensure that at least one of the candidate next NBA states (i.e., the ones that can decrease the distance to \mathcal{V}_F) can be reached. Based on these two observations, we conclude that such a sequence \mathbf{e} will be generated, completing the proof. \blacksquare

Note that the graph \mathcal{G} is agnostic to the structure of the environment, meaning that an edge in \mathcal{G} may not be able to be traversed. For instance, consider an edge in this graph that is enabled only if the robot applies a certain action to a movable object that is in a region blocked by fixed obstacles; in this case the continuous-time controller will not be able to execute this action due to the environmental structure. Satisfaction of the second assumption in Proposition 1 implies that if such scenarios never happen, (e.g., all regions and objects that the robot needs to interact with are accessible and the continuous-time controller allows the robot to reach them) then the proposed hybrid control method will satisfy the assigned LTL task if this formula is feasible. However, if the second assumption does not hold, there may be an alternative sequence of automaton states to follow in order to satisfy the LTL formula that the proposed algorithm failed to find due to the a-priori unknown structure of the environment.

APPENDIX II
REACTIVE CONTROLLER OVERVIEW

This Appendix provides a brief description of the reactive, vector field controller from [6] used in this work. As shown in Fig. 3, the robot navigates the physical space and discovers obstacles (e.g., using the semantic mapping engine in [45]), which are dilated by the robot radius and stored in the semantic space. Potentially overlapping obstacles in the semantic space are subsequently consolidated in real time to form the mapped space. A change of coordinates \mathbf{h} from this space is then employed to construct a geometrically simplified (but topologically equivalent) model space, by merging familiar obstacles overlapping with the boundary of the enclosing freespace to this boundary, deforming other familiar obstacles to disks, and leaving unknown obstacles intact. It is shown in [6] that the constructed change of coordinates $\mathbf{h}^{\mathcal{I}}$ between the mapped and the model space, for a given index set \mathcal{I} of instantiated familiar obstacles, is a C^∞ diffeomorphism away from sharp corners. Using the diffeomorphism $\mathbf{h}^{\mathcal{I}}$, we construct a hybrid vector field controller (with the modes indexed by \mathcal{I} , i.e., depending on external perceptual updates), that guarantees simultaneous obstacle avoidance and target convergence, while respecting input command limits, in unexplored semantic environments (see [6, Eq. (1)]). The reactive controller is further extended to accommodate differential-drive robot dynamics, while maintaining the same formal guarantees.

APPENDIX III
DESCRIPTION OF THE TOPOLOGY CHECKING
ALGORITHM

This Appendix includes an algorithmic outline of the topology checking algorithm from Section V-A, shown in Algorithm 1. This algorithm works as follows. Starting with the initially assumed polygonal enclosing freespace \mathcal{F}_e for either the robot or the robot-object pair, we subtract the union of all known dilated movable objects in \mathcal{M} and fixed obstacles in $\mathcal{P}_{\mathcal{I}}$ (corresponding to the index set \mathcal{I} of localized familiar obstacles), using standard logic operations with polygons (see e.g., [46]–[48]). This operation results in a list of freespace components, which we denote by $\mathcal{L}_{\mathcal{F}} := (\mathcal{F}_1, \mathcal{F}_2, \dots)$. From this list, we identify the freespace \mathcal{F} as the freespace component \mathcal{F}_k that contains the robot position \mathbf{x} (or the robot-object pair center $\mathbf{x}_{i,c}$) and re-define the enclosing freespace as its convex hull, i.e., $\mathcal{F}_e := \text{Conv}(\overline{\mathcal{F}_k})$.

If the goal \mathbf{x}^* is contained in \mathcal{F}_e , the reactive controller proceeds as usual, using \mathcal{F}_e for the diffeomorphism construction (see Appendix II), and treating all other freespace components as obstacles. Otherwise, we need to check whether movable objects or fixed obstacles cause a freespace disconnection that does not allow for successful action completion. Namely, we need to check whether both the robot position \mathbf{x} (or the robot-object pair center $\mathbf{x}_{i,c}$) and the target \mathbf{x}^* are included in the same connected component of the set $\mathcal{L}_{\mathcal{F}+\mathcal{M}} := (\bigcup_i \mathcal{F}_i) \cup (\bigcup_j \mathcal{M}_j)$, i.e., the union

of all freespace components in $\mathcal{L}_{\mathcal{F}}$ with all dilated movable objects in \mathcal{M} . This would imply that a subset of movable objects in \mathcal{M} blocks the target configuration. In that case, the robot switches to the Fix mode to rearrange these objects; otherwise, the interface layer reports to the symbolic controller that the current action is infeasible.

In the former case, we proceed one step further to identify the blocking movable objects in order to reconfigure them on-the-fly. First, we isolate the connected components of the union of all movable objects in \mathcal{M} into a list $\mathcal{L}_{\mathcal{M}} := (\mathcal{M}_1, \mathcal{M}_2, \dots)$; we refer to the elements of that list as the *movable object clusters*. Assuming that each movable object cluster is connected to at most two freespace components from $\mathcal{L}_{\mathcal{F}}$, we build a connectivity tree rooted at the robot’s (or the robot-object pair’s) freespace \mathcal{F} , by checking whether the closures of two individual regions overlap; the tree’s vertices are geometric regions (freespace components in $\mathcal{L}_{\mathcal{F}}$ and movable object clusters in $\mathcal{L}_{\mathcal{M}}$) and edges denote adjacency. We then backtrack from the vertex of the tree that contains the goal \mathbf{x}^* until we reach the root, saving the encountered movable object clusters along the way. Any movable object intersecting any of these clusters is pushed to a stack of *blocking movable objects* $\mathcal{B}_{\mathcal{M}}$.

REFERENCES

- [1] C. R. Garrett, T. Lozano-Perez, and L. P. Kaelbling, “Sampling-based methods for factored task and motion planning,” *The International Journal of Robotics Research*, vol. 37, no. 13-14, pp. 1796–1825, 2018.
- [2] W. Vega-Brown and N. Roy, “Asymptotically optimal planning under piecewise-analytic constraints,” in *The 12th International Workshop on the Algorithmic Foundations of Robotics*, 2016.
- [3] A. Krontiris and K. Bekris, “Dealing with difficult instances of object rearrangement,” in *Robotics: Science and Systems*, 2015.
- [4] S. Srivastava, E. Fang, L. Riano, R. Chitnis, S. Russell, and P. Abbeel, “Combined task and motion planning through an extensible planner-independent interface layer,” in *IEEE International Conference on Robotics and Automation*, 2014, pp. 639–646.
- [5] K. He, M. Lahijanian, L. E. Kavraki, and M. Y. Vardi, “Towards manipulation planning with temporal logic specifications,” in *IEEE International Conference on Robotics and Automation*, 2015, pp. 346–352.
- [6] V. Vasilopoulos, G. Pavlakos, S. L. Bowman, J. D. Caporale, K. Daniilidis, G. J. Pappas, and D. E. Koditschek, “Reactive Semantic Planning in Unexplored Semantic Environments Using Deep Perceptual Feedback,” *IEEE Robotics and Automation Letters*, vol. 5, no. 3, pp. 4455–4462, 2020.
- [7] J. E. Hopcroft, J. T. Schwartz, and M. Sharir, “On the Complexity of Motion Planning for Multiple Independent Objects; PSPACE-Hardness of the “Warehouseman’s Problem”,” *The International Journal of Robotics Research*, vol. 3, no. 4, pp. 76–88, 1984.
- [8] E. Rimon and D. E. Koditschek, “Exact Robot Navigation Using Artificial Potential Functions,” *IEEE Transactions on Robotics and Automation*, vol. 8, no. 5, pp. 501–518, 1992.
- [9] L. L. Whitcomb, D. E. Koditschek, and J. B. D. Cabrera, “Toward the Automatic Control of Robot Assembly Tasks via Potential Functions: The Case of 2-D Sphere Assemblies,” in *IEEE International Conference on Robotics and Automation*, 1992, pp. 2186–2192.
- [10] C. S. Karagoz, H. I. Bozma, and D. E. Koditschek, “Coordinated Navigation of Multiple Independent Disk-Shaped Robots,” *IEEE Transactions on Robotics*, vol. 30, no. 6, p. 1289–1304, December 2014.
- [11] H. Isil Bozma and D. E. Koditschek, “Assembly as a noncooperative game of its pieces: analysis of 1D sphere assemblies,” *Robotica*, vol. 19, no. 01, pp. 93–108, 2001.
- [12] C. S. Karagoz, H. I. Bozma, and D. E. Koditschek, “Feedback-based event-driven parts moving,” *IEEE Transactions on Robotics*, vol. 20, no. 6, pp. 1012–1018, 2004.

Algorithm 1 Topology Checking Algorithm.

```
function TOPOLOGYCHECKING( $\mathbf{x}, \mathbf{x}^*, \mathcal{F}_e, \mathcal{M}, \mathcal{P}_I$ )  
   $\mathcal{L}_{\mathcal{F}} \leftarrow \text{Subtract}(\mathcal{F}_e, \text{Union}(\mathcal{M}, \mathcal{P}_I))$   
  for  $\mathcal{F}_k \in \mathcal{L}_{\mathcal{F}}$  do  
    if  $\mathbf{x} \in \mathcal{F}_k$  then  
       $\mathcal{F} \leftarrow \mathcal{F}_k$   
       $\mathcal{F}_e \leftarrow \text{Conv}(\overline{\mathcal{F}_k})$   
      break  
    end if  
  end for  
  if  $\mathbf{x}^* \in \mathcal{F}$  then  
     $\mathcal{B}_{\mathcal{M}} \leftarrow \emptyset$   $\triangleright$  No blocking objects or obstacles  
     $\text{IsFeasible} \leftarrow \text{True}$   $\triangleright$  Task feasible  
  else  
     $\mathcal{L}_{\mathcal{F}+\mathcal{M}} \leftarrow (\bigcup_i \mathcal{F}_i) \cup (\bigcup_j \mathcal{M}_j), \mathcal{F}_i \in \mathcal{L}_{\mathcal{F}}, \mathcal{M}_j \in \mathcal{M}$   
    for  $\mathcal{F}_k \in \mathcal{L}_{\mathcal{F}+\mathcal{M}}$  do  
      if  $\mathbf{x} \in \mathcal{F}_k$  then  
        if  $\mathbf{x}^* \in \mathcal{F}_k$  then  
           $\mathcal{L}_{\mathcal{M}} \leftarrow \bigcup_j \mathcal{M}_j, \mathcal{M}_j \in \mathcal{M}$   
           $(\mathcal{V}_{\mathcal{L}}, \mathcal{E}_{\mathcal{L}}) \leftarrow \text{ConnectTree}(\mathcal{L}_{\mathcal{F}}, \mathcal{L}_{\mathcal{M}})$   
          for  $V \in \mathcal{V}_{\mathcal{L}}$  do  
            if  $\mathbf{x}^* \in V$  then  
               $\mathcal{B}_{\mathcal{M}} \leftarrow \text{BacktrackFrom}(V)$   
              break  
            end if  
          end for  
           $\text{IsFeasible} \leftarrow \text{True}$   
        else  
           $\mathcal{B}_{\mathcal{M}} \leftarrow \emptyset$   $\triangleright$  Blocked by fixed obstacles  
           $\text{IsFeasible} \leftarrow \text{False}$   
        end if  
      break  
    end if  
  end for  
  end if  
  return  $\mathcal{F}_e, \text{IsFeasible}, \mathcal{B}_{\mathcal{M}}$   
end function
```

- [13] O. Arslan, D. P. Guralnik, and D. E. Koditschek, "Coordinated robot navigation via hierarchical clustering," *IEEE Transactions on Robotics*, vol. 32, no. 2, p. 352–371, 2016.
- [14] J. van den Berg, M. Stilman, J. Kuffner, M. Lin, and D. Manocha, "Path planning among movable obstacles: A probabilistically complete approach," in *The 8th International Workshop on the Algorithmic Foundations of Robotics*, 2010.
- [15] G. Konidaris, L. P. Kaelbling, and T. Lozano-Perez, "From Skills to Symbols: Learning Symbolic Representations for Abstract High-Level Planning," *Journal of Artificial Intelligence Research*, vol. 61, pp. 215–289, 2018.
- [16] W. Vega-Brown and N. Roy, "Admissible abstractions for near-optimal task and motion planning," in *International Joint Conference on Artificial Intelligence*, 2018.
- [17] J. Wolfe, B. Marthi, and S. Russell, "Combined task and motion planning for mobile manipulation," in *International Conference on Automated Planning and Scheduling*, 2010.
- [18] W. Vega-Brown and N. Roy, "Anchoring abstractions for near-optimal task and motion planning," in *RSS Workshop on Integrated Task and Motion Planning*, 2017.
- [19] M. Stilman and J. Kuffner, "Planning Among Movable Obstacles with Artificial Constraints," *The International Journal of Robotics Research*, vol. 27, no. 11-12, pp. 1295–1307, 2008.

- [20] H.-N. Wu, M. Levihn, and M. Stilman, "Navigation Among Movable Obstacles in unknown environments," in *IEEE/RSJ International Conference on Intelligent Robots and Systems*, 2010, pp. 1433–1438.
- [21] M. Levihn, J. Scholz, and M. Stilman, "Planning with movable obstacles in continuous environments with uncertain dynamics," in *IEEE International Conference on Robotics and Automation*, 2013, pp. 3832–3838.
- [22] M. Guo, K. H. Johansson, and D. V. Dimarogonas, "Revising motion planning under linear temporal logic specifications in partially known workspaces," in *IEEE International Conference on Robotics and Automation*, 2013, pp. 5025–5032.
- [23] M. Guo and D. V. Dimarogonas, "Multi-agent plan reconfiguration under local ltl specifications," *The International Journal of Robotics Research*, vol. 34, no. 2, pp. 218–235, 2015.
- [24] M. R. Maly, M. Lahijanian, L. E. Kavraki, H. Kress-Gazit, and M. Y. Vardi, "Iterative temporal motion planning for hybrid systems in partially unknown environments," in *The 16th International Conference on Hybrid Systems: Computation and Control*, 2013, pp. 353–362.
- [25] M. Lahijanian, M. R. Maly, D. Fried, L. E. Kavraki, H. Kress-Gazit, and M. Y. Vardi, "Iterative temporal planning in uncertain environments with partial satisfaction guarantees," *IEEE Transactions on Robotics*, vol. 32, no. 3, pp. 583–599, 2016.
- [26] S. C. Livingston, R. M. Murray, and J. W. Burdick, "Backtracking temporal logic synthesis for uncertain environments," in *IEEE International Conference on Robotics and Automation*, 2012, pp. 5163–5170.
- [27] S. C. Livingston, P. Prabhakar, A. B. Jose, and R. M. Murray, "Patching task-level robot controllers based on a local μ -calculus formula," in *IEEE International Conference on Robotics and Automation*, 2013, pp. 4588–4595.
- [28] H. Kress-Gazit, G. E. Fainekos, and G. J. Pappas, "Temporal-logic-based reactive mission and motion planning," *IEEE Transactions on Robotics*, vol. 25, no. 6, pp. 1370–1381, 2009.
- [29] J. Alonso-Mora, J. A. DeCastro, V. Raman, D. Rus, and H. Kress-Gazit, "Reactive mission and motion planning with deadlock resolution avoiding dynamic obstacles," *Autonomous Robots*, vol. 42, no. 4, pp. 801–824, 2018.
- [30] N. Piterman, A. Pnueli, and Y. Sa'ar, "Synthesis of reactive (1) designs," in *International Workshop on Verification, Model Checking, and Abstract Interpretation*. Springer, 2006, pp. 364–380.
- [31] C. Belta, V. Isler, and G. J. Pappas, "Discrete abstractions for robot motion planning and control in polygonal environments," *IEEE Transactions on Robotics*, vol. 21, no. 5, pp. 864–874, 2005.
- [32] G. Pola, A. Girard, and P. Tabuada, "Approximately bisimilar symbolic models for nonlinear control systems," *Automatica*, vol. 44, no. 10, pp. 2508–2516, 2008.
- [33] V. Vasilopoulos, G. Pavlakos, K. Schmeckpeper, K. Daniilidis, and D. E. Koditschek, "Reactive Navigation in Partially Familiar Planar Environments Using Semantic Perceptual Feedback," *Under review, arXiv: 2002.08946*, 2020.
- [34] O. Arslan and D. E. Koditschek, "Sensor-Based Reactive Navigation in Unknown Convex Sphere Worlds," *The International Journal of Robotics Research*, vol. 38, no. 1-2, pp. 196–223, July 2018.
- [35] Y. Shoukry, P. Nuzzo, A. L. Sangiovanni-Vincentelli, S. A. Seshia, G. J. Pappas, and P. Tabuada, "SMC: Satisfiability Modulo Convex Programming," *Proceedings of the IEEE*, vol. 106, no. 9, pp. 1655–1679, 2018.
- [36] G. E. Fainekos, H. Kress-Gazit, and G. J. Pappas, "Hybrid controllers for path planning: A temporal logic approach," in *44th IEEE Conference on Decision and Control, European Control Conference, (CDC-ECC)*, Seville, Spain, 2005, pp. 4885–4890.
- [37] C. Baier and J.-P. Katoen, *Principles of Model Checking*. MIT Press, Cambridge, MA, 2008.
- [38] M. Kloetzer and C. Belta, "A Fully Automated Framework for Control of Linear Systems from Temporal Logic Specifications," *IEEE Transactions on Automatic Control*, vol. 53, no. 1, pp. 287–297, 2008.
- [39] Y. Kantaros, M. Malencia, V. Kumar, and G. J. Pappas, "Reactive temporal logic planning for multiple robots in unknown environments," in *2020 IEEE International Conference on Robotics and Automation (ICRA)*. IEEE, 2020, pp. 11 479–11 485.
- [40] Y. Kantaros and M. M. Zavlanos, "Stylus*: A temporal logic optimal control synthesis algorithm for large-scale multi-robot systems," *The International Journal of Robotics Research*, vol. 39, no. 7, pp. 812–836, 2020.
- [41] V. Vasilopoulos, W. Vega-Brown, O. Arslan, N. Roy, and D. E. Koditschek, "Sensor-Based Reactive Symbolic Planning in Partially

- Known Environments,” in *IEEE International Conference on Robotics and Automation*, 2018, pp. 5683–5690.
- [42] R. W. Brockett, “Asymptotic stability and feedback stabilization,” in *Differential Geometric Control Theory*. Birkhauser, 1983, pp. 181–191.
- [43] P. Gastin and D. Oddoux, “Fast ltl to büchi automata translation,” in *International Conference on Computer Aided Verification*. Springer, 2001, pp. 53–65.
- [44] A. Bisoffi and D. V. Dimarogonas, “A hybrid barrier certificate approach to satisfy linear temporal logic specifications,” in *American Control Conference*, 2018, pp. 634–639.
- [45] S. L. Bowman, N. Atanasov, K. Daniilidis, and G. J. Pappas, “Probabilistic data association for semantic SLAM,” in *IEEE Int. Conf. Robotics and Automation*, May 2017, pp. 1722–1729.
- [46] H. ElGindy, H. Everett, and G. T. Toussaint, “Slicing an ear using prune-and-search,” *Pattern Recognition Letters*, vol. 14, no. 9, pp. 719–722, 1993.
- [47] E. Clementini, P. D. Felice, and P. van Oosterom, “A Small Set of Formal Topological Relationships Suitable for End-User Interaction,” *Advances in Spatial Databases*, pp. 277–295, 1993.
- [48] D. H. Douglas and T. K. Peucker, “Algorithms for the Reduction of the Number of Points Required to Represent a Digitized Line or its Caricature,” *Cartographica: The International Journal for Geographic Information and Geovisualization*, vol. 10, pp. 112–122, 1973.